Journal of Crystal Growth 499 (2018) 18–23

Contents lists available at ScienceDirect

Journal of Crystal Growth

journal homepage: www.elsevier.com/locate/jcrysgro

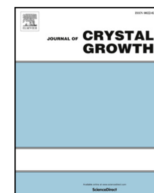

Effect of growth temperature on the structural and optoelectronic properties of epitaxial indium oxide films

Xuejian Du*, Baoyuan Man

School of Physics and Electronics, Shandong Normal University, Jinan 250358, PR China

ARTICLE INFO

Communicated by R. Bhat

Keywords:
A1. X-ray diffraction
A3. Metal–organic chemical vapor deposition
B1. Oxides
B2. Semiconducting materials

ABSTRACT

High quality monocrystalline indium oxide (In_2O_3) films have been epitaxially grown on SiO_2 (0001) substrates by the metal-organic chemical vapor deposition (MOCVD) method. The influences of different growth temperatures on the structural, morphological and optoelectronic properties of the films were studied in detail. The film deposited at 650 °C exhibited the narrowest X-ray linewidth with an epitaxial relationship of In_2O_3 (1 1 1)‖SiO_2 (0001). The highest Hall mobility of 27.84 $cm^2 V^{-1} s^{-1}$ with a minimum carrier concentration of $5.03 \times 10^{19} cm^{-3}$ and a minimum resistivity of $4.24 \times 10^{-3} \Omega$ cm was obtained for the film prepared at 650 °C. The average transmittance for all the samples in the visible range exceeded 82% and the optical band gap of the films was calculated about 3.7 eV.

1. Introduction

Indium oxide (In_2O_3) is an outstanding n-type transparent oxide semiconductor (TOS) which is drawn considerable attention owing to the coexistence of excellent electrical and optical properties [1–3]. The common body-centered cubic (bcc-, a = 10.118 Å) In_2O_3 with a wide band gap of ~3.7 eV has been extensively applied in optoelectronic devices, solar cells, catalysts, gas sensors and so on [4–8]. Numerous physical and chemical methods have been used to prepare In_2O_3 films, such as magnetron sputtering [9], sol-gel process [10], electrochemical deposition [11], etc. However, most of the obtained In_2O_3 films are nano- or poly-crystalline structures via the methods mentioned above. The low-quality films are susceptible to many other factors, such as a high concentration of defects as well as surface adsorbates, which hinders the fabrication of high performance In_2O_3-based devices. Therefore, the preparation of high-quality In_2O_3 films should be emphasized to meet the increasingly higher requirements.

To date, several works related to the growth of single crystal In_2O_3 films on various substrates have been reported. Among these studies, epitaxial In_2O_3 films were grown on sapphire [12] or Y-stabilized ZrO_2 [13] by molecular beam epitaxy (MBE), as well as on InAs, MgO [14] or glass [15] by pulsed laser deposition (PLD), respectively. However, there are very few reports on the growth of epitaxial In_2O_3 films on the SiO_2 (0001) substrates, especially by use of MOCVD. Single crystal SiO_2 possesses a hexagonal structure with lattice constants of a = 4.914 Å and c = 5.405 Å; and the crystal lattice mismatch between the In_2O_3 (such as [1 1 1] orientation, $\sqrt{2}\,a_{In_2O_3}$ = 14.307 Å) and SiO_2 ([0 0 1] orientation, $3a_{SiO_2}$ = 14.742 Å) is calculated at 2.95% [16]. Besides, the commercially available SiO_2 wafer is low cost and easy to obtain, which is perfectly suitable as a substrate material for the growth of In_2O_3 films. In this paper, high-quality single crystal In_2O_3 films were successfully deposited on the SiO_2 (0001) substrates by MOCVD. Structural, morphological and optoelectronic properties of the films were investigated in detail.

2. Experimental details

The epitaxial growth of In_2O_3 films on SiO_2 (0001) substrates was carried out using a high-vacuum vertical MOCVD system. The stainless steel reactor was a cold wall chamber, and its diameter and height were about 25 cm. The SiO_2 substrates were bought from an optics and fine mechanics company. The SiO_2 substrates (20 × 20 × 0.5 mm) were cut as small pieces (10 × 10 × 0.5 mm) by a diamond glass cutter. And then the SiO_2 substrates were successively cleaned by anhydrous alcohol, acetone, and deionized water in an ultrasonic bath prior to deposition. The cleaned substrates were subsequently blow-dried by high purity N_2 (5 N in purity). Commercially available trimethylindium (TMI) and high purity O_2 (5 N) were used as organometallic (OM) and oxygen sources, respectively. The OM source was stored in a stainless bubbler which was kept at 15 °C with a pressure of 600 torr. Ultra high purity N_2 (9 N), used as the carrier gas, passed through the OM bubbler and saturated with TMI vapor to the reactor. The reactor adopted a dual

* Corresponding author.
E-mail address: dxjsdnu@163.com (X. Du).

https://doi.org/10.1016/j.jcrysgro.2018.07.033
Received 22 March 2018; Received in revised form 27 July 2018; Accepted 30 July 2018
Available online 31 July 2018
0022-0248/ © 2018 Elsevier B.V. All rights reserved.

airflow mode, that is, the OM source steam and the oxygen moved pass the substrate by horizontal flow and vertical flow, respectively. During the deposition period (300 min), the flow rates of TMI, O_2 and N_2 were set at 3, 50 and 400 standard cubic centimeters per minute (sccm), respectively. The flow velocity of gas in the reactor was calculated at about 1.54×10^{-4} m/s. The growth temperatures were set at 570, 610, 650 and 690 °C, respectively, and the growth pressure was fixed at 20 torr.

The crystalline structures of the obtained films were examined using a Bruker D8 Advance X-ray diffractometer with Cu Kα1 (λ = 1.5406 Å) radiation. High-resolution transmission electron microscopy (HRTEM) and the selected-area electron diffraction (SAED) measurements were performed to study the microstructure of the sample on a Tecnai F30 transmission electron microscope. The surface morphologies of the films were examined by means of a Zeiss merlin compact scanning electron microscope (SEM). The chemical composition of the prepared film was measured by the X-ray photoelectron spectroscopy (XPS) technique performed on the ESCALAB MK II multi-technique electron spectrometer. An East Changing ET9000 Hall measurement system was employed to determine the electrical properties of the films. The transmittance measurements were performed on a TU-1901 double-beam UV–Vis-NIR spectrophotometer in the wavelength range of 200–800 nm.

3. Results and discussion

Fig. 1(a)–(e) shows the representative XRD patterns of the SiO_2 substrate (as comparison) and the samples deposited with different growth temperatures. The thicknesses of the films prepared at 570, 610, 650 and 690 °C are respectively about 83, 115, 127 and 100 nm by SEM measurement (not shown here). Correspondingly, the growth rates of the In_2O_3 films are 0.28, 0.38, 0.42 and 0.33 nm/min. As can be seen from Fig. 1, only one prominent peak located at 30.64° apart from the substrate SiO_2 (0003) peak, which is corresponding to the bixbyite In_2O_3 (2 2 2) reflection, can be detected for all the samples. It is worth noting that the location of the In_2O_3 (2 2 2) peak shifts slightly to a larger angle compared with the No. 06-0416 card of Joint Committee on Powder Diffraction Standards (JCPDS). Due to the lattice parameter

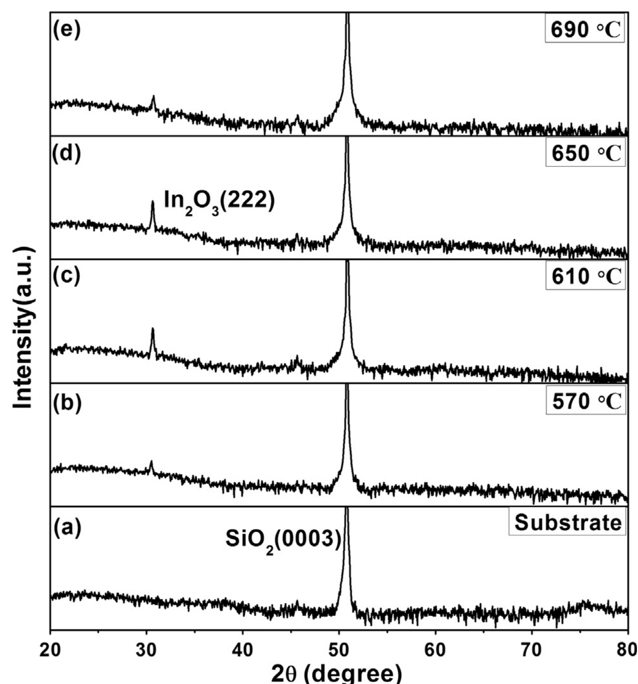

Fig. 1. XRD patterns of the SiO_2 substrate and samples with different growth temperatures.

of the film (14.307 Å) is smaller than that of the substrate (14.742 Å), the biaxial tension will exist in the film during the epitaxial growth. The existence of the in-plane tension can cause the film to undergo an out-plane contraction, which leads to the shift of the In_2O_3 (2 2 2) peak to a higher angle. Besides, the weak and obscure peak at 45.64° may be ascribed to the substrate impurity (such as SiO) or the instrument noise. The results imply that the obtained samples are pure In_2O_3 films of bixbyite structure with a single orientation along In_2O_3 [1 1 1] direction. The full width at half maximum (FWHM) of the In_2O_3 (2 2 2) peak are 0.46°, 0.35°, 0.23° and 0.43° corresponding to curve (b), (c), (d) and (e), respectively. Besides, the intensity of the In_2O_3 (2 2 2) peak increases at first and then decreases as the growth temperature rises, with a largest intensity obtained at 650 °C. These results indicate that the structure of the In_2O_3 films is appreciably affected by the growth temperature and the sample deposited at 650 °C presents the highest degree of crystallinity.

The microstructure of the prepared film was further investigated by means of TEM measurements. Fig. 2(a)–(c) respectively demonstrates the cross-sectional image of low magnification TEM, HRTEM and SAED patterns for the sample deposited at 650 °C. From Fig. 2(a), a distinct interface between the In_2O_3 film and the SiO_2 substrate with a film thickness of about 127 nm can be observed. The HRTEM image shown in Fig. 2(b) exhibits a uniformly intact lattice plane for the film. Besides, the as-marked interplanar spacing is calculated as 0.293 ± 0.005 nm, which is corresponding to the bbc-In_2O_3 (2 2 2) plane. This value is very close to that determined from XRD (~0.292 nm). These results indicate that the obtained In_2O_3 film possesses a uniformly single-crystalline structure and the growth orientation is along In_2O_3 [1 1 1]. Moreover, due to the SiO_2 substrate material is damaged by the electron beam through the TEM measurement operated at 300 kV, hence the lattice of the substrate cannot be detected [16]. The surface of the SiO_2 material suffers damage under the high energy electron irradiation, and the structure of the SiO_2 substrate may vary from monocrystalline to mixed monocrystalline and polycrystalline. From the SAED pattern shown in Fig. 2(c), a representative single-crystalline diffraction pattern can be observed clearly. Besides, the as-marked diffraction spots are corresponding to In_2O_3 (2 2 2), SiO_2 (0001) and SiO_2 (1 0 1) planes, confirming the growth orientation of [1 1 1] for the In_2O_3 film. As noted in Fig. 2(c), the In_2O_3 (2 2 2), SiO_2 (0001) diffraction spots and the center point are in a line, indicating the In_2O_3 (2 2 2) plane is aligned to the SiO_2 substrate. The HRTEM and SAED results reveal an evident epitaxial relationship of In_2O_3 (1 1 1)‖SiO_2 (0001), which is in accordance with the XRD analyses.

The surface morphologies of the In_2O_3 films with different growth temperatures of 570, 610, 650 and 690 °C are shown in Fig. 3. A compact surface with small uniform island-like grains and well-defined grains boundaries is observed in Fig. 3(a). The size of the grains becomes larger in Fig. 3(b), indicating an improvement in the film crystallinity. In Fig. 3(c), obviously angular grains with the largest grain size as well as inerratic and distinct boundaries are observed among all the samples, implying the best crystallization of the film deposited at 650 °C. From Fig. 3(d), the grain size of the film is reduced obviously as well as the grain boundary becomes anomalous with some pinholes detected, indicating the film crystallinity degrades dramatically. Based on the SEM images, the mean grain sizes of the films prepared at 570, 610, 650 and 690 °C are estimated to be 25.8, 40.5, 72.2 and 31.4 nm, respectively. The results further illustrate that the growth temperature has an impact on the crystallinity of the In_2O_3 films and the optimal growth temperature is confirmed to be 650 °C.

The XPS technique was employed to verify the chemical composition of the obtained films. All the XPS spectra are calibrated by use of the C 1s peak located at 284.8 eV. Fig. 4(a) displays the survey spectrum of the obtained film deposited at 650 °C, in which the peaks corresponding to C 1s, O 1s, In 3p, In 3d and In 4d core levels can be observed without any other elements signals. The C 1s peak is mainly ascribed to the presence of adventitious hydrocarbon contamination.

Download English Version:

https://daneshyari.com/en/article/8148353

Download Persian Version:

https://daneshyari.com/article/8148353

Daneshyari.com